Journal of Applied Polymer Science

Anisotropy of the elastic modulus for hybrid composites reinforced by short fibers and particles with respect to material porosity

Hong-Liang Dai,[1,2] Chao Mei,[1,2] Yan-Ni Rao[1,2]

[1]State Key Laboratory of Advanced Design and Manufacturing for Vehicle Body, Hunan University, Changsha 410082, China
[2]Department of Engineering Mechanics, College of Mechanical and Vehicle Engineering, Hunan University, Changsha 410082, China
Correspondence to: H.-L. Dai (E-mail: hldai520@sina.com)

ABSTRACT: Hybrid composites reinforced by short fibers and particles (HCRSFPs) have been widely used in many fields, and more and more scholars are paying attention to hybrid composites. In this study, the elastic moduli of HCRSFPs in arbitrarily chosen directions were investigated with respect to their porosities. A material model was built with the assumption of a compound of particles and polymer matrix containing voids as an effective matrix, and the HCRSFPs were treated as the compound of short fibers and the effective matrix. With consideration of the three-dimensional spatial orientation distribution and the length distribution of the short fibers, the laminate analog approach and the Halpin–Tsai model were used to predict the elastic moduli of the HCRSFPs. Numerical examples and analyses showed that the fiber orientation distribution, reinforcement volume fraction, and porosity had great effects on the elastic moduli of the HCRSFPs. © 2016 Wiley Periodicals, Inc. J. Appl. Polym. Sci. **2016**, *133*, 43708.

KEYWORDS: composites; fibers; porous materials

Received 29 October 2015; accepted 28 March 2016
DOI: 10.1002/app.43708

INTRODUCTION

Hybrid composites reinforced by short fibers and particles (HCRSFPs), which have low weights and outstanding mechanical properties, have been used extensively in many domains, including automotive, aircraft, and sports equipment. HCRSFPs contain pure polymers such as polypropylene, short fibers such as glass fibers or carbon fibers, and spherical inorganic particles. Hybrid composites reinforced by multiple reinforcements can create a synergetic effect; this is usually called a *hybrid effect*.[1] For example, hybrid composites reinforced by multiple reinforcements can have better mechanical properties than composites reinforced by a single reinforcement;[2] this is called the *positive hybrid effect*. *Porosity*, which is defined as air-filled cavities inside an otherwise continuous material, is an often unavoidable part of all composites, and it is essential for reliable model predictions of mechanical properties.[3] Porosity in HCRSFPs is such a noticeable factor that due attention should be paid to theoretical and practical research.

A lot of studies have been done on the mechanical properties of hybrid composites. By studying the flexural behavior through both experiments and finite element analysis, Dong and Davies[4] found out the optimal design for the flexural behavior of glass and carbon fiber-reinforced polymer hybrid composites. Later, they[5] derived the flexural and tensile moduli of unidirectional hybrid epoxy composites reinforced by S-2 glass and T700S carbon fibers on the basis of classic lamination theory. According to a two-phase composite material theoretical model, Duc and Minh[6] gave the six elastic constants first and then presented a method to determine the bending deflection of three-phase polymer composite plates consisting of reinforced glass fibers and titanium oxide particles. By conducting experiments, Fu and Lauke[7] found that the replacement of a part of the polymer matrix by calcite particles for fiber composites to obtain hybrid composites led to a further increase in the tensile modulus. Microcomputed tomography was used by Lee *et al.*[8] to observe the three-dimensional structure of fibers in the composite to acquire the fiber length distribution and fiber orientation distribution. Then, the effective elastic modulus for a multiphase hybrid composite was derived. Alamri and Low[9] fabricated and investigated an epoxy system reinforced with either recycled cellulose fibers or nanosiliconcarbide particles and with both recycled cellulose fibers and nanosiliconcarbide. They found that the influence of the addition of nanosiliconcarbide to recycled cellulose fiber/epoxy composites on the mechanical properties was positive with respect to the toughness properties.

The elastic modulus plays an important role in the mechanical properties. Therefore, large number of researchers have done numerous studies on the elastic moduli of composites. Theocaris

and Sideridis[10] made three assumptions: (1) filler particles are spherical, (2) fillers are completely dispersed, and (3) the volume fraction of fillers is sufficiently small. These assumptions allowed them to neglect any interaction among fillers. Then, they derived a theoretical expression for the elastic modulus of particulate composites. Later, Sideridis[11] developed a theoretical expression for the transverse elastic modulus in fiber-reinforced composites through the assumption that the composite material consists of three phases, that is, the fiber, the matrix, and the interphase. On the basis of a micromechanical model of a short-inorganic-fiber-reinforced polymer composite, Liang[12] presented an expression for the Young's modulus of short-inorganic-fiber-reinforced polymer composites. On the basis of statistics, Meng *et al.*[13] investigated the effects of unequal compressive and tensile moduli on carbon fiber-reinforced plastic composites, and they proposed that strain-dominated failure criteria should be used for composite design, testing, and certification. By virtue of Maxwell's concept of equivalent inhomogeneity, Mogilevskaya *et al.*[14] evaluated the effective elastic modulus of a fiber-reinforced, unidirectional composite with isotropic phases.

The elastic modulus, especially the longitudinal modulus of the composite, has been investigated very much at this point. On the basis of a laminate analogy approach and the shear lag model, Fu and Lauke[15] presented an expression for the longitudinal modulus of misaligned short-fiber-reinforced polymers. Epaarachchi *et al.*[16] proposed a simplified approach for the analysis of the longitudinal modulus and other mechanical properties of randomly distributed short-fiber composites. Many studies of the anisotropy of the elastic moduli of composites have been done. By taking their previous work a step further, Fu and Lauke[17] later presented a method for analyzing the anisotropy of the elastic moduli of misaligned short-fiber-reinforced polymers. According to the laminate analogy and modified Tsai–Hill criteria, Mortazavian and Fatemi[18] investigated the effects of the fiber orientation and anisotropy on the elastic modulus of a short-fiber-reinforced polymer composite. In terms of the porosity, Madsen *et al.*[19] included the influence of the porosity on the composite stiffness on the basis of a modified rule of mixtures, and a maximum obtainable stiffness of the composites was calculated at a certain transition fiber weight fractions by their theory.

However, with the consideration of porosity, the elastic modulus of a hybrid composite simultaneously reinforced by short fibers and particles in arbitrarily chosen directions has not been studied up to this point, and this was the main purpose of our research reported in this article.

DESCRIPTION OF THE PROBLEM

Three-Dimensional Spatial Fiber Distribution

In the process of injection molding and extrusion, short fibers are often damaged and broken by the actions of shear, extrusion, and impact. As a result, the lengths of the fibers will inevitably become unequal, and the orientations of the fibers will be different. The distribution of short fiber length and short fiber orientation can be described by certain probability density functions.

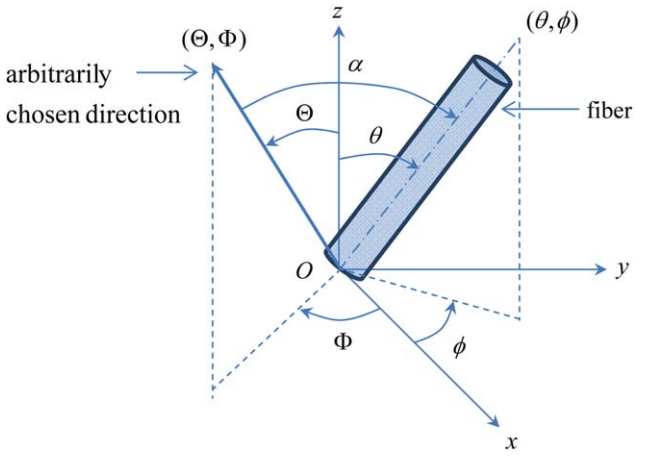

Figure 1. Description of a single short fiber's orientation (θ, ϕ) and an arbitrarily chosen direction (Θ, Φ). *O coordinate origin.* [Color figure can be viewed in the online issue, which is available at wileyonlinelibrary.com.]

Fiber Length Distribution. The Weibull distribution function has been widely used by many researchers to describe the fiber length distribution. However, fiber breakage is severe in multiphase hybrid composites, and the use of the Weibull distribution function to describe short-fiber distribution will cause a relatively large deviation. The log-normal function matches the experimental statistics better than the Weibull distribution function.[20] Hence, the log-normal function is supposed to be most suitable for HCRSFPs. The log-normal distribution function [$f(L)$] can be expressed as follows[20]:

$$f(L)=\frac{1}{n\sqrt{2\pi}L}\exp\left[-\frac{(\ln L-m)^2}{2n^2}\right] \tag{1}$$

where m and n are the mean and standard deviation, respectively, and L is the fiber length. From eq. (1), the mean fiber length (L_{mean}) can be defined as follows:

$$L_{mean}=\int_0^\infty Lf(L)dL \tag{2}$$

Fiber Orientation Distribution. A three-dimensional coordinate system was adopted to show the orientation of a certain short fiber. It can be described by only two parameters, θ and ϕ,[21] where θ is the angle that the fiber's axis makes with the z axis and ϕ is the angle that the projection of fiber's axis to plane xOy makes with the x axis. Angles Θ and Φ, which describe the arbitrarily chosen directions, can be defined in the same way (see Figure 1). The probability density function of θ [$g_1(\theta)$] and the probability density function of ϕ [$g_2(\phi)$] are given as follows[22]:

$$g_1(\theta)=\frac{(\sin\theta)^{2p-1}(\cos\theta)^{2q-1}}{\int_{\theta_{min}}^{\theta_{max}}(\sin\theta)^{2p-1}(\cos\theta)^{2q-1}d\theta}\quad\left(0\le\theta_{min}\le\theta\le\theta_{max}\le\frac{\pi}{2}\right) \tag{3}$$

$$g_2(\phi)=\frac{|\sin\phi|^{2s-1}|\cos\phi|^{2t-1}}{\int_{\theta_{min}}^{\theta_{max}}|\sin\phi|^{2s-1}|\cos\phi|^{2t-1}d\phi}\quad(0\le\phi_{min}\le\phi\le\phi_{max}\le2\pi) \tag{4}$$

where p, q, s, and t are shape parameters that can determine the shape of the distribution curve. As in different molding

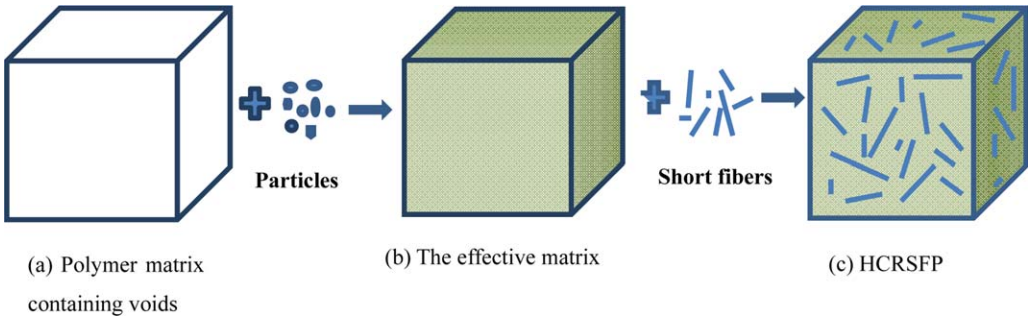

Figure 2. Process of building the material model. [Color figure can be viewed in the online issue, which is available at wileyonlinelibrary.com.]

situations, the distributions of the fiber orientation will be different, the distribution of fiber orientation has to be described by the distribution functions $g_1(\theta)$ and $g_2(\phi)$ with different parameters.

Material Model

For HCRSFPs, a novel micromechanical model is proposed in this article. The voids, whose volume fraction (V_v) is the porosity, can be treated as a phase of the HCRSFPs. So, there are four phases in HCRSFPs, namely, the pure polymer, the voids, the particles, and the short fibers. The voids distribute uniformly in the pure polymer, and their shapes are considered to be spherical or quasi-spherical, so the mechanical properties of a compound consisting of voids and pure polymer can be regarded as isotropic. Such a compound is defined as a polymer matrix containing voids. Similarly, as the particles distribute randomly and evenly in the polymer matrix containing voids and their shapes are roughly considered to be spherical, the mechanical properties of a particle-filled polymer matrix containing voids are taken to be isotropic, too. This particle-filled polymer matrix containing voids is defined as an effective matrix. Finally, HCRSFPs can be treated as short-fiber-filled effective matrixes. The building process of the material model is shown in Figure 2.

It is obvious that the summation of each phase's volume fraction is 1, as follows:

$$V_{pp} + V_p + V_f + V_v = 1$$

where V_{pp} is the volume fraction of the pure polymer, V_p is the particle volume fraction, and V_f is the fiber volume fraction.

Polymer Matrix Containing Voids

There are two phases in the polymer matrix: the pure polymer and the voids. The relative V_{pp} and relative voids are $\frac{V_{pp}}{V_{pp}+V_v}$ and $\frac{V_v}{V_{pp}+V_v}$, respectively. The volume fraction of the polymer matrix containing voids (V_m) is calculated as follows:

$$V_m = V_{pp} + V_v \tag{6}$$

The elastic modulus and the Poisson ratio of a polymer matrix containing voids (E_m and μ_m, respectively) can be obtained by the law of mixture:

$$E_m = \frac{V_{pp}}{V_m} E_{pp} \tag{7}$$

$$\mu_m = \frac{V_{pp}}{V_m} \mu_{pp} \tag{8}$$

where E_{pp} and μ_{pp} are the elastic modulus and Poisson ratio of the pure polymer, respectively.

Effective Matrix

There are three phases in the effective matrix, they are the pure polymer, the voids, and the particles. The volume fraction of the effective matrix (V_0) can be expressed as follows:

$$V_0 = V_m + V_p \tag{9}$$

The relative volume fractions of the polymer matrix containing voids and particles are V_m/V_0 and V_p/V_0, respectively. On the basis of the theory of the Halpin–Tsai model,[23] the elastic modulus of the effective matrix (E_0) can be calculated as follows:

$$E_0 = \frac{E_m\left(1+2\lambda_p\eta\frac{V_p}{V_0}\right)}{1-\eta\frac{V_p}{V_0}} \tag{10}$$

where

$$\eta = \frac{\frac{E_p}{E_m}-1}{\frac{E_p}{E_m}+2\lambda_p} \tag{11}$$

where E_p and λ_p are the elastic modulus and the aspect ratio of the particles, respectively. As mentioned previously, the shape of the particles could be roughly considered to be spherical, so the aspect ratio was taken as $\lambda_p \approx 1$.

The Poisson ratio of the effective matrix (μ_0) can be calculated by another form of the law of mixture.[24] It is shown as follows:

$$\mu_0 = \frac{\mu_m\mu_p}{\mu_p\frac{V_m}{V_0}+\mu_m\frac{V_p}{V_0}} \tag{12}$$

where μ_p is the Poisson ratio of the particles.

SOLUTION TO THE PROBLEM

Laminate Analog Approach (LAA)

According to the LAA, HCRSFPs can be divided into a large number of laminas. As the particles are distributed randomly and uniformly in the hybrid composite, the distributions of the particles in each laminate are considered to be the same. However, the distributions of the fibers in each lamina are different. Each lamina contains short fibers with lengths between l and $l + dl$, with orientations between θ and $\theta + d\theta$ and ϕ and $\phi + d\phi$.

Table I. Comparison of the Elastic Modulus Values Predicted by This Study and Reference 25

				$E_{(\pi/2,\ 0)}$ (GPa)		
No.	V_f	V_p	V_v	Predictions in this study	Predictions in ref. 25	Experimental data in ref. 25[a]
1	6.0	0	8.2	4.28	4.4	3.8 (±0.4)
2	12.6	0	6.7	6.01	6.1	6.1 (±0.4)
3	19.8	0	13.7	7.16	7.4	6.8 (±1.1)

[a] The data in parentheses are standard deviations.
"$E_{(\pi/2,0)}$" is the value of the elastic modulus in the direction $(\Theta, \Phi) = (\pi/2,0)$.

Take a certain lamina, for example. The certain lamina contains fibers with lengths between l_0 and $l_0 + dl$ and orientations between θ_0 and $\theta_0 + d\theta$ and ϕ_0 and $\phi_0 + d\phi$. In the coordinate system of this laminate (i.e., the local coordinate system), the longitudinal elastic modulus (E_{11}), whose direction is parallel to the fibers' direction, can be given as follows[23]

$$E_{11} = \frac{E_0\left(1+2\lambda_f\eta_1 V_f\right)}{1-\eta_1 V_f} \tag{13}$$

where λ_f is the aspect ratio of the fibers [$\lambda_f = 1/d_f$ (where d_f is the diameter of the fibers)] and η_1 is given as follows:

$$\eta_1 = \frac{\frac{E_f}{E_0}-1}{\frac{E_f}{E_0}+2\lambda_f} \tag{14}$$

where E_f is Young's modulus of the fibers. The transverse modulus (E_{22}) and the in-plane shear modulus (G_{12}), which are not sensitive to the aspect ratio of a fiber, can be denoted as follows:[23]

$$E_{22} = \frac{E_0\left(1+2\eta_2 V_f\right)}{1-\eta_2 V_f} \tag{15}$$

$$G_{12} = \frac{G_0\left(1+\eta_3 V_f\right)}{1-\eta_3 V_f} \tag{16}$$

where

$$\eta_2 = \frac{\frac{E_f}{E_0}-1}{\frac{E_f}{E_0}+2} \quad \text{and} \quad \eta_3 = \frac{\frac{G_f}{G_0}-1}{\frac{G_f}{G_0}+1} \tag{17}$$

where G_f is the shear modulus of the fibers and G_0 is the shear modulus of the effective matrix. G_0 can be expressed as follows:

$$G_0 = \frac{E_0}{2(1+\mu_0)}$$

The longitudinal Poisson ratio (μ_{12}) can be obtained by the rule of mixture:

$$\mu_{12} = \mu_0 V_0 + \mu_f V_f \tag{18}$$

where μ_f is the Poisson ratio of the fibers. The transverse Poisson ratio (μ_{21}) can be given as follows:

$$\mu_{21} = \frac{\mu_{12} E_{22}}{E_{11}} \tag{19}$$

Elastic Modulus of the HCRSFPs in an Arbitrarily Chosen Direction

Now, an arbitrary direction (Θ, Φ) is chosen, and the elastic modulus in this direction [$E_{(\Theta,\Phi)}$] will be predicted. To obtain the transformation equation that relates the local coordinate system of the lamina to the global coordinate system, α is defined as the angle that the fibers of angle (θ, ϕ) make with the arbitrarily chosen direction (Θ, Φ; see Figure 1). The relationship of α, θ, ϕ, Θ, and Φ is shown as follows:

$$\cos\alpha = \cos\theta\cos\Theta + \sin\theta\sin\Theta\cos(\phi - \Phi) \tag{20}$$

Thus, the transformed stiffness matrix in the global coordinate system ($\overline{\mathbf{Q}}_{\mathbf{ij}}$) can be gained by the following equation:

$$\begin{pmatrix} \overline{\mathbf{Q}}_{11} \\ \overline{\mathbf{Q}}_{22} \\ \overline{\mathbf{Q}}_{12} \\ \overline{\mathbf{Q}}_{66} \\ \overline{\mathbf{Q}}_{16} \\ \overline{\mathbf{Q}}_{26} \end{pmatrix} = \begin{pmatrix} a^4 & b^4 & 2a^2b^2 & 4a^2b^2 \\ b^4 & a^4 & 2a^2b^2 & 4a^2b^2 \\ a^2b^2 & a^2b^2 & a^4+b^4 & -4a^2b^2 \\ a^2b^2 & a^2b^2 & -2a^2b^2 & (a^2-b^2)^2 \\ a^3b & -ab^3 & ab^3-a^3b & 2(ab^3-a^3b) \\ ab^3 & -a^3b & a^3b-ab^3 & 2(a^3b-ab^3) \end{pmatrix} \times \begin{pmatrix} \mathbf{Q}_{11} \\ \mathbf{Q}_{22} \\ \mathbf{Q}_{12} \\ \mathbf{Q}_{66} \end{pmatrix} \tag{21}$$

where $a = \cos\alpha$, $b = \sin\alpha$, and $\mathbf{Q_{ij}}$ is the stiffness matrix that relates the stress to the strain in the local coordinate system of a lamina. Because there is a continuous fiber length distribution and a continuous fiber orientation distribution, the overall laminate stiffness matrix ($\overline{A}_{ij}$) can be obtained through the integration of the fiber length and orientation:

$$\overline{\mathbf{A}}_{\mathbf{ij}} = \int_{L_{\min}}^{L_{\max}} \int_{\theta_{\min}}^{\theta_{\max}} \int_{\phi_{\min}}^{\phi_{\max}} \overline{\mathbf{Q}}_{\mathbf{ij}} f(L) g_1(\theta) g_2(\phi) dL d\theta d\phi \tag{22}$$

Finally, $E_{(\Theta,\ \Phi)}$ can be gained from the $\overline{\mathbf{A}}_{\mathbf{ij}}$ components:

$$E_{(\Theta,\Phi)} = \frac{\overline{A}_{11}\overline{A}_{22} - \overline{A}_{12}^2}{\overline{A}_{22}} \tag{23}$$

NUMERICAL EXAMPLES

Example 1

To validate the theory in this article, we made comparison to the work conducted by Camacho *et al.*,[25] who explored the elastic modulus of composites reinforced by multiple fibers and microspheres. Camacho *et al.* provided prediction data and experimental data of the elastic moduli of composites containing short quartz fibers and voids. Even though the V_p value of these composites was equal to zero, they still took the porosity, which is the main concern of this study, into consideration.

The data from Camacho *et al.* were as follows: $E_{pp} = 3.3$ GPa, $\mu_{pp} = 0.29$, $E_f = 69$ GPa, $\mu_f = 0.17$, $d_f = 9$ μm, and

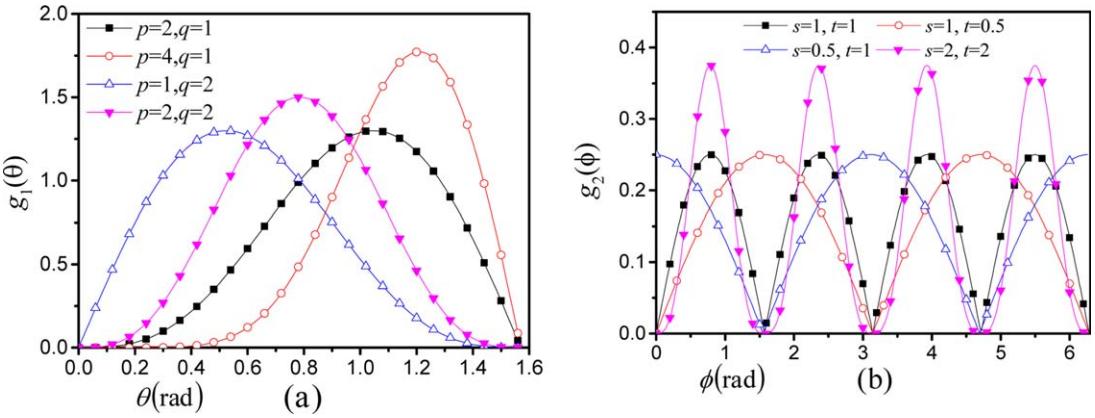

Figure 3. Probability density distribution functions of fiber orientation with different parameters: (a) $g_1(\theta)$ $(0 \le \theta \le \pi/2)$ and (b) $g_2(\phi)$ $(0 \le \phi \le 2\pi)$. [Color figure can be viewed in the online issue, which is available at www.interscience.wiley.com.]

$L_{mean} = 6.4$ mm ($m = 8.65$, $n = 0.48$). Camacho *et al.* used an orientation average (a_{ij}) to describe the distribution of short fibers. They tested three specimens: (1) $a_{33} = 0.006$ (corresponding to $\theta_{mean} = 1.56$), (2) $a_{33} = 0.013$ ($\theta_{mean} = 1.55$), and (3) $a_{33} = 0.027$ ($\theta_{mean} = 1.54$). These three data indicate that the fiber distributions of all of these three specimens were slightly nonplanar and uniformly distributed in the plane *xOy*.[25] The following parameters were taken to correspond with the fiber distributions of the three specimens: $s = 0.5$, $t = 0.5$, (1) $p = 1000$, $q = 0.6$, (2) $p = 800$, $q = 0.6$, and (3) $p = 500$, $q = 0.6$. In their experiment, the in-plane (i.e., plane *xOy*) elastic modulus was tested, so the value of Θ in this study was taken as $\Theta = \pi/2$, correspondingly. Because the fibers in the specimens distributed uniformly in the plane, the value of Φ could be taken randomly. We took it as $\Phi = 0$. The predictions and experimental data from Camacho *et al.* and the predictions from this study are shown in Table I. As shown in Table I, we found that the results were in good agreement, and the correctness of the theory in this study is further explained. The advantage of the model put forward in this study over the model of Camacho *et al.* is that our model can predict the elastic modulus in any direction of a composite, whereas the model of Camacho *et al.* can only predict the elastic modulus in a specified direction of a composite. Moreover, a different form of law of mixture [see eq. (12)] was used in this study to calculate μ_0 because this form of law of mixture has been argued to be more suitable for the prediction of the Poisson ratio of particle-reinforced composites.[24] However, in the work of Camacho *et al.*, a form similar to eq. (18) was adopted. As a result, our predictions of the elastic modulus of the composites in this example were closer to the experimental data than those of Camacho *et al.* Our predictions were about 2.4% lower than the predictions of Camacho *et al.*

Example 2: The Results of Four Situations

In the example, the parameters of the components in the composite were chosen as follows, $E_{pp} = 2.5$ GPa, $\mu_{pp} = 0.35$, $G_{pp} = \frac{E_{pp}}{2(1+\mu_{pp})}$, $V_{pp} = 0.58$, $V_v = 0.02$, $E_p = 200$ GPa, $\mu_p = 0.25$, $V_p = 0.2$, $E_f = 70$ GPa, $\mu_f = 0.25$, $G_f = \frac{E_f}{2(1+\mu_f)}$, $V_f = 0.2$, $d_f = 12$ μm, $m = 5$, and $n = 0.5$.

Figure 3 shows the orientation distribution functions $g_1(\theta)$ and $g_2(\phi)$ with a range of $0 \le \theta \le \pi/2$ and $0 \le \phi \le 2\pi$, respectively. As shown in Figure 3, different shape parameters resulted in different shapes of the distribution function curve; this means that different molding situations of the hybrid composites resulted in different distributions of short fibers. When $g_1(\theta)$ or $g_2(\phi)$ had a high value at a certain value of θ or ϕ, this indicated that there were lots of fibers located in this direction. On the contrary, when $g_1(\theta)$ or $g_2(\phi)$ had a low value at a certain value of θ or ϕ, it indicated that there were not many fibers located in this direction.

Figure 4 displays the elastic modulus distribution of the HCRSFPs for four situations. The four pictures in Figure 4 are the corresponding modulus distributions for the four situations of fiber orientation distribution in Figure 3, where (a) $p = 2$, $q = 1$, $s = 1$, and $t = 1$; (b) $p = 4$, $q = 1$, $s = 1$, and $t = 0.5$; (c) $p = 1$, $q = 2$, $s = 0.5$, and $t = 1$; and (d) $p = 2$, $q = 2$, $s = 2$, and $t = 2$. As shown in Figure 4, the elastic moduli were diverse for different directions. The distributions of the elastic modulus were diverse for different fiber orientation distributions. The elastic modulus was symmetric about $\Phi = \pi$ for the range $0 \le \Phi \le 2\pi$ and symmetric about $\Phi = \pi/2$ for the range $0 \le \Phi \le \pi$. This was because the distribution of ϕ was symmetric about $\phi = \pi$ for the range $0 \le \phi \le 2\pi$ and symmetric about $\phi = \pi/2$ for the range $0 \le \phi \le \pi$. When we compared the four pictures with each other, this showed that the fiber orientation distribution not only influenced the distribution of the elastic modulus but also influenced the maximum value of the elastic modulus. For example, the maximum in situation c was greater than the maximum in situation a. Short fibers were inclined to orient in some directions for each of the four situations; as a result, the elastic modulus in these directions had the highest value. For situation a, the maximum of the elastic modulus appeared to be at about $\theta = 1$ and $\phi = \pi/4$, $3\pi/4$, $5\pi/4$, and $7\pi/4$. From all of the four situations, it was revealed that when $\Theta = 0$, the elastic modulus was a constant, regardless of changes in Φ. This phenomenon was explained in ref. 15. Figure 4 reveals the significant influence of the fiber orientation distribution on the elastic modulus in different directions.

Example 3

In this example, the parameters of the fiber orientation distribution function were taken as $p = 2$, $q = 1$, $s = 1$, and $t = 1$. Because of the symmetry, the elastic modulus had the

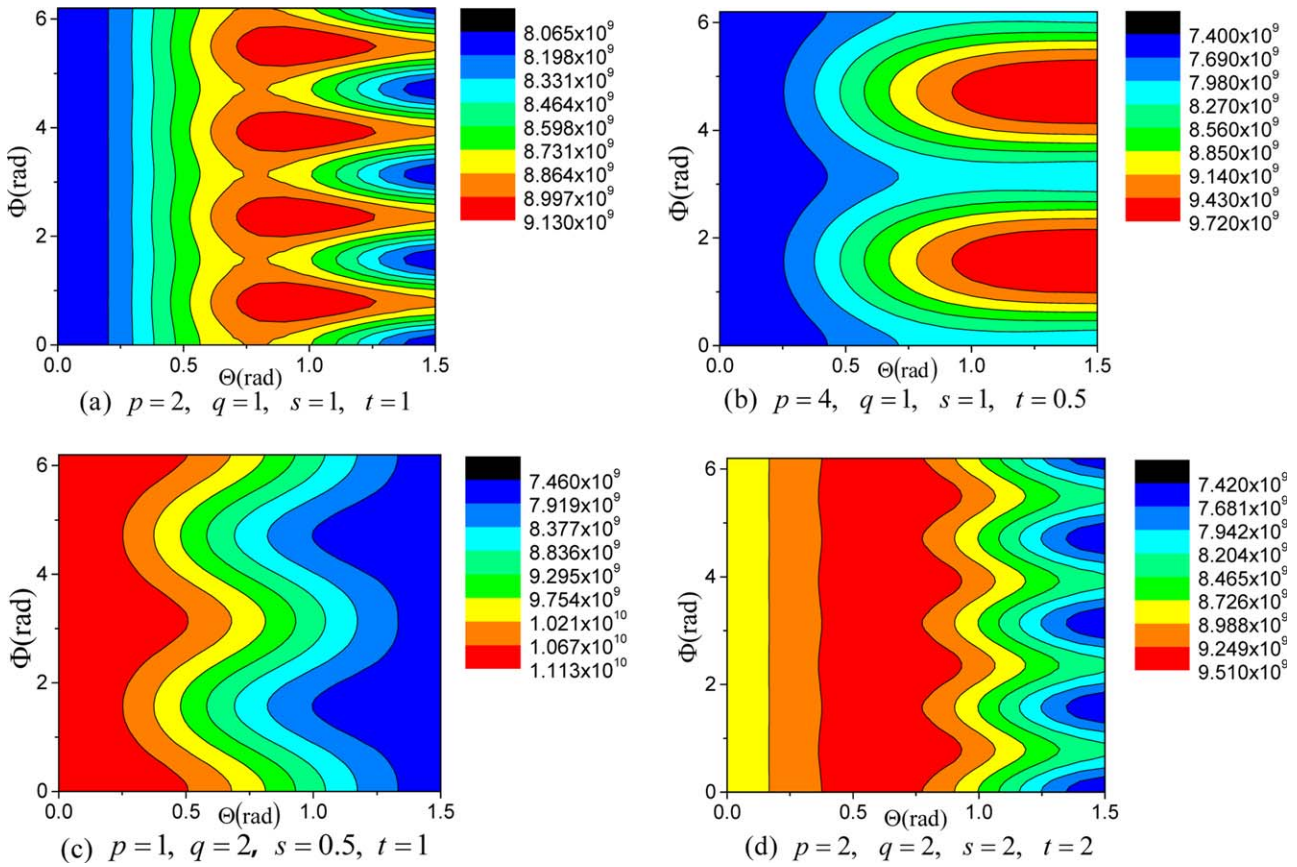

Figure 4. Elastic modulus distribution of HCRSFPs with different parameters. [Color figure can be viewed in the online issue, which is available at wileyonlinelibrary.com.]

maximum value in four directions, regardless of changes in each component's volume fraction [see Figure 4(a)]. One of the four directions was figured out; the direction was $(\Theta_{max}, \Phi_{max}) = (0.9553, 0.7854)$. Next, the influence of each component's volume fraction on the elastic modulus is discussed. In example 3, the porosity (V_v) was taken as several constants, V_p and V_f were variables, and $V_{pp} = 1 - V_p - V_f - V_v$. The other data were the same as those in example 2.

The influence of the porosity (V_v) is demonstrated in Figure 5. The value of the elastic modulus in the maximum direction [$E_{(\Theta_{max},\Phi_{max})}$] was amplified with the enlargement of the reinforcement volume fraction ($V_f + V_p$), and it was amplified more and more rapidly when $V_f + V_p$ became large. $E_{(\Theta_{max},\Phi_{max})}$ was smaller when the HCRSFPs contained a higher porosity (V_v). As shown in Figure 5, the porosity was an important factor in the determination of the elastic modulus, and the negative effect of voids in the HCRSFPs cannot be ignored in the practical engineering applications.

Figure 6 shows the elastic modulus variation with the fiber volume fraction (V_f) for diverse V_ps in the maximum direction ($\Theta = \Theta_{max}$, $\Phi = \Phi_{max}$). The elastic modulus increased with V_f for all four situations: $V_p = 0.1$, $V_p = 0.2$, $V_p = 0.3$, and $V_p = 0.4$. The maximum $V_f + V_p$ was 0.8 (i.e., $V_f + V_p \leq 0.8$). When V_f was the same, the elastic modulus of the composite with a higher V_p increased more quickly than that with a lower V_p, for there were more reinforcements (short fibers and particles) in the composite when V_p was higher. We concluded that the more reinforcements there were, the more obvious the reinforcing effect was. When $V_f + V_p = 0.8$, the elastic modulus with $V_p = 0.2$ had the highest value among the four situations. This phenomenon, which is related to the optimal design, is discussed in the following section.

Figure 7 shows the $E_{(\Theta_{max},\Phi_{max})}$ ($\Theta = \Theta_{max}$, $\Phi = \Phi_{max}$) variation with V_p for diverse V_fs. We found that the elastic modulus

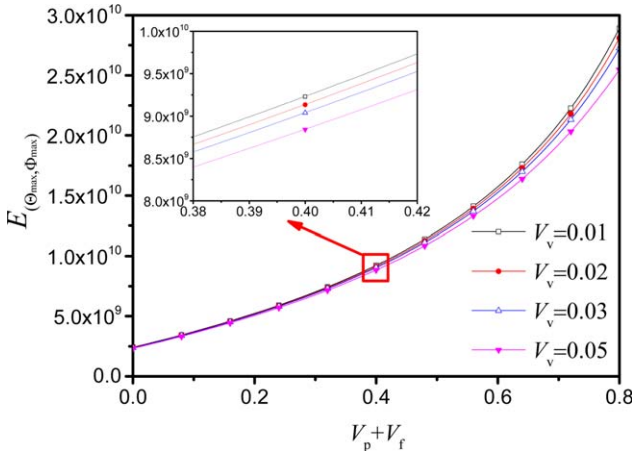

Figure 5. $E_{(\Theta_{max},\Phi_{max})}$ ($\Theta = \Theta_{max}$, $\Phi = \Phi_{max}$) variation with changing $V_p + V_f$ values for diverse values of porosity (V_v). [Color figure can be viewed in the online issue, which is available at wileyonlinelibrary.com.]

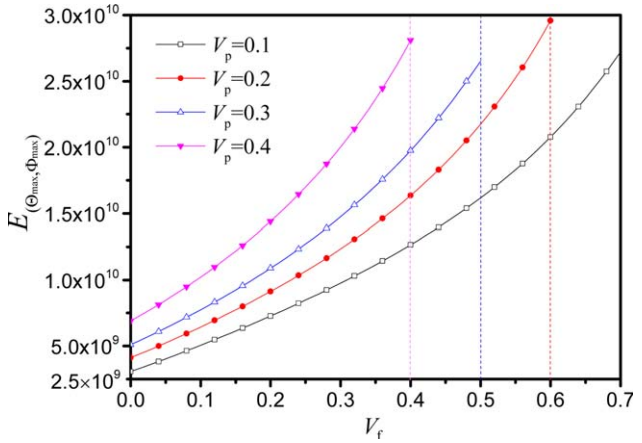

Figure 6. $E_{(\Theta_{max},\Phi_{max})}$ ($\Theta = \Theta_{max}$, $\Phi = \Phi_{max}$) variation with V_f for diverse V_p values ($V_v = 0.05$). [Color figure can be viewed in the online issue, which is available at wileyonlinelibrary.com.]

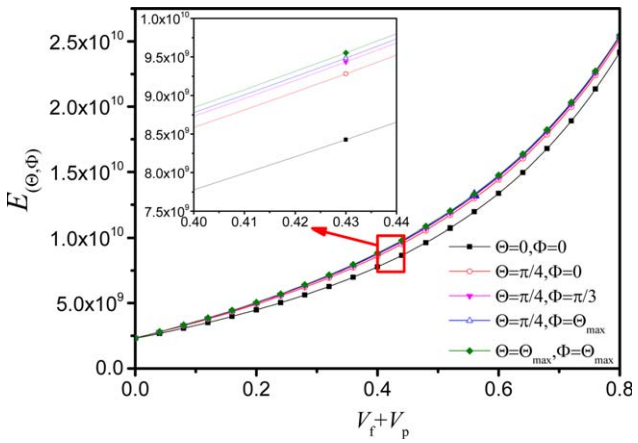

Figure 8. Elastic modulus variation in different directions with the total $V_f + V_p$ ($V_f = V_p$, $V_v = 0.05$). [Color figure can be viewed in the online issue, which is available at wileyonlinelibrary.com.]

increased with increasing V_p for all four situations: $V_f = 0.1$, $V_f = 0.2$, $V_f = 0.3$, and $V_f = 0.4$. Similar to Figure 6, when V_p was the same, the elastic modulus with a higher V_f augmented faster than that with a lower V_f. When $V_f + V_p = 0.8$, the elastic moduli with $V_f = 0.1$ and $V_f = 0.4$ were relatively higher.

The elastic modulus in different directions is shown in Figure 8. In the reinforcements, there were one-half short fibers and another half particles, that is, $V_f = V_p$. The elastic modulus increased with increasing $V_f + V_p$. For a relatively low volume fraction (ca. $0 \le V_f + V_p \le 0.2$), the modulus increased relatively slowly, whereas for a relatively high volume fraction (ca. $0.6 \le V_f + V_p \le 0.8$), the modulus increased relatively quickly. For an arbitrarily chosen direction, when Θ was the same ($\Theta = \pi/4$), the modulus in the direction $\Phi = \Phi_{max}$ was larger than that in the direction $\Theta = \pi/3$ and the direction $\Phi = 0$ at the same value of $V_f + V_p$; when Φ was the same ($\Phi = \Phi_{max}$), the modulus in direction $\Theta = \Theta_{max}$ was larger than that in the direction $\Theta = \pi/4$ at the same value of $V_f + V_p$. Obviously, we figured out that the maximum elastic modulus appeared in the direction (Θ_{max}, Φ_{max}).

Figure 9 shows the $E_{(\Theta_{max},\Phi_{max})}$ ($\Theta = \Theta_{max}$, $\Phi = \Phi_{max}$) variation with the changing of $V_f + V_p$ in three situations: the changing of V_f when $V_p = 0$, the changing of V_p when $V_f = 0$, and the changing of $V_f + V_p$ ($V_f = V_p$). The modulus increased with the increment of $V_f + V_p$, no matter whether the composite was reinforced by one reinforcement only or by both reinforcements. When $0.675 \le V \le 0.870$, the composite reinforced by two reinforcements had a higher elastic modulus than composite reinforced by only one reinforcement; this is the so-called positive hybrid effect. When $V \le 0.675$, the composite reinforced only by short fibers possessed the highest elastic modulus. When $V \ge 0.870$, the composite reinforced only by particles possessed the highest elastic modulus.

As we have discussed which values of $V_f + V_p$ generated a positive hybrid effect, we move a step forward to study the question of when a positive hybrid effect is generated in two-reinforcement-reinforced composites, what the percentage of short fibers to the two reinforcements would possess the maximal modulus. Figure 10 reveals the $E_{(\Theta_{max},\Phi_{max})}$ ($\Theta = \Theta_{max}$, $\Phi = \Phi_{max}$) variation with changing in $\frac{V_f}{V_f + V_p}$. It is interesting to

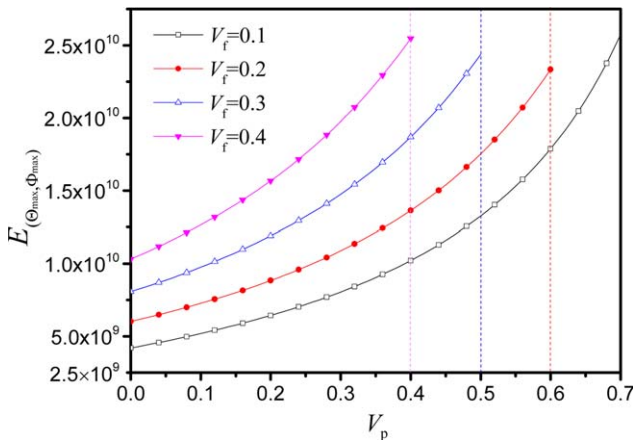

Figure 7. $E_{(\Theta_{max},\Phi_{max})}$ ($\Theta = \Theta_{max}$, $\Phi = \Phi_{max}$) variation with V_p for diverse V_f values ($V_v = 0.05$). [Color figure can be viewed in the online issue, which is available at wileyonlinelibrary.com.]

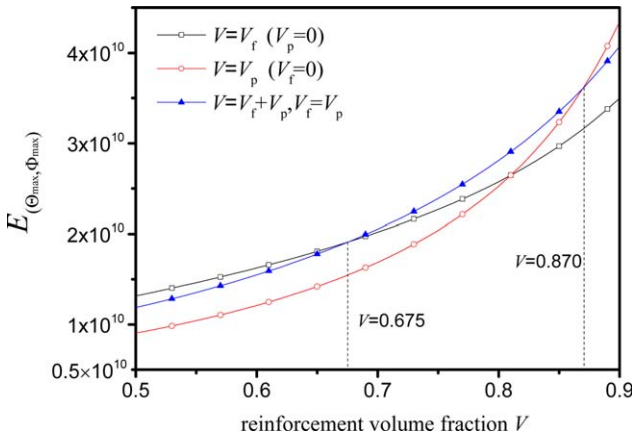

Figure 9. $E_{(\Theta_{max},\Phi_{max})}$ ($\Theta = \Theta_{max}$, $\Phi = \Phi_{max}$) variation with changing values of $V_f + V_p$ for three situations ($V_v = 0.02$). [Color figure can be viewed in the online issue, which is available at wileyonlinelibrary.com.]

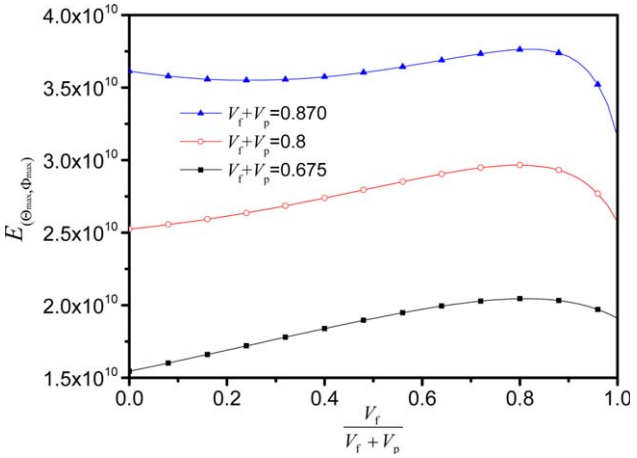

Figure 10. $E_{(\Theta_{max},\Phi_{max})}$ ($\Theta = \Theta_{max}$, $\Phi = \Phi_{max}$) variation with changing $\frac{V_f}{V_f+V_p}$ ($V_v = 0.02$). [Color figure can be viewed in the online issue, which is available at wileyonlinelibrary.com.]

note that when about $\frac{V_f}{V_f+V_p}=0.8$, the maximums of the elastic modulus for all the three situations ($V_p + V_f = 0.675$, $V_p + V_f = 0.8$, and $V_p + V_f = 0.870$) were obtained; this indicated that there was an optimal percentage of short fibers to the two reinforcements in terms of a positive hybrid effect. Thus, when the data from the short fibers, particles, and polymer are known and the direction in which the modulus will be predicted has been chosen, one can find out the optimal proportion of each component in the composite to obtain the largest elastic modulus with the theory in this study.

CONCLUSIONS

In this study, the mechanical properties of the polymer matrix and the matrix effect were derived by the Halpin–Tsai model and the law of mixture. Classical LAA was used in this study. For a single lamina of the HCRSFPs, the Halpin–Tsai model was used to predict the modulus. Finally, the expression of the elastic modulus of the HCRSFPs was obtained. The advantage of our developed model took into consideration the influence of the porosity, which exists universally in composite materials. The model in our work provides a microscope of how voids influence the elastic modulus of composites in the initial step of derivation.

The main results and findings of this study are as follows:

1. The fiber orientation distribution has a significant influence on the elastic modulus in different orientations of the HCRSFPs. Different fiber orientation distributions will not only cause huge differences of the elastic modulus distribution but will also influence the maximum of the elastic modulus.
2. For all directions, the elastic modulus increases with increasing $V_f + V_p$.
3. In a certain range of $V_f + V_p$, composites reinforced by two reinforcements have a higher elastic modulus than composites reinforced by only one reinforcement.
4. Furthermore, a certain proportion of two reinforcements will generate a maximum elastic modulus; this is helpful for the design of a composite in practical applications.
5. Voids in the composite can cause a decrease in the elastic modulus, and the porosity should draw enough attention during engineering applications.

ACKNOWLEDGMENTS

The authors gratefully acknowledge the support of National Natural Science Foundation of China (11372105), New Century Excellent Talents Program in University (NCET-13-0184), State Key Laboratory of Advanced Design and Manufacturing for Vehicle Body (71475004) and Hunan Provincial Innovation Foundation for Postgraduate (CX2014B156).

REFERENCES

1. Peled, A.; Mobasher, B.; Cohen, Z. *Cem. Concr. Compos.* **2009**, *31*, 647.
2. Dong, C.; Ranaweera-Jayawardena, H. A.; Davies, I. *J. Compos. B* **2012**, *43*, 573.
3. Madsen, B.; Thygesen, A.; Lilholt, H. *Compos. Sci. Technol.* **2007**, *67*, 1584.
4. Dong, C.; Davies, I. *J. Mater. Des.* **2012**, *37*, 450.
5. Dong, C.; Davies, I. *J. Mater. Des.* **2014**, *54*, 893.
6. Duc, N. D.; Minh, D. K. *Comput. Mater. Sci.* **2010**, *49*, S194.
7. Fu, S. Y.; Lauke, B. *Compos. A* **1998**, *29*, 575.
8. Lee, D. J.; Oh, H.; Song, Y. S.; Youn, J. R. *Compos. Sci. Technol.* **2012**, *72*, 278.
9. Alamri, H.; Low, I. M. *J. Appl. Polym. Sci.* **2012**, *126*, E221.
10. Theocaris, P. S.; Sideridis, E. *J. Appl. Polym. Sci.* **1984**, *29*, 2997.
11. Sideridis, E. *J. Appl. Polym. Sci.* **1993**, *48*, 243.
12. Liang, J. Z. *Compos. B* **2012**, *43*, 1763.
13. Meng, M.; Le, H. R.; Rizvi, M. J.; Grove, S. M. *Compos. Struct.* **2015**, *126*, 207.
14. Mogilevskaya, S. G.; Kushch, V. I.; Stolarski, H. K.; Crouch, S. L. *Int. J. Solids Struct.* **2013**, *50*, 4161.
15. Fu, S. Y.; Lauke, B. *Compos. Sci. Technol.* **1998**, *58*, 389.
16. Epaarachchi, J.; Ku, H.; Gohel, K. *J. Compos. Mater.* **2010**, *44*, 779.
17. Fu, S. Y.; Lauke, B. *Compos. Sci. Technol.* **1998**, *58*, 1961.
18. Mortazavian, S.; Fatemi, A. *Compos. B* **2015**, *72*, 116.
19. Madsen, B.; Thygesen, A.; Lilholt, H. *Compos. Sci. Technol.* **2009**, *69*, 1057.
20. Lee, D. J.; Hwang, S. H.; Song, Y. S.; Youn, J. R. *Polym. Test.* **2015**, *41*, 99.
21. Avérous, L.; Quantin, J. C.; Crespy, A. *Polym. Eng. Sci.* **1997**, *37*, 329.
22. Xia, M.; Hamada, H.; Maekawa, Z. *Int. Polym. Process.* **1995**, *10*, 74.
23. Halpin, J. C.; Kardos, J. L. *Polym. Eng. Sci.* **1976**, *16*, 344.
24. Theocaris, P. S. In The Mesophase Concept in Composites; Henrici-Olivé, G., Olivé, S., Eds.; Springer: Berlin, **1987**; p 16.
25. Camacho, C. W.; Tucker, C. L.; Yalvaç, S.; McGee, R. L. *Polym. Compos.* **1990**, *11*, 229.

SGML and CITI Use Only
DO NOT PRINT